Effect of Nitrogen Atoms and Grain Boundaries on Shear Properties of Graphene by Molecular Dynamics Simulations

Shingo Okamoto and Akihiko Ito

***Abstract*—We investigated the shear properties of graphene containing nitrogen atoms and grain boundaries (GBs) via molecular dynamics (MD) simulations. In the MD simulation, we used two types of potential functions: the second–generation reactive empirical bond order (REBO) potential for covalent C–C bonds and the Tersoff potential for covalent C–N bonds. The effects of nitrogen content and different distributions of nitrogen atoms in graphene on its properties were studied. It was found that a nitrogen content of up to 4 % had little effect on the shear properties of graphene except when two nitrogen atoms contained in graphene adjoined each other. In addition, the shear strength depends more greatly on GBs than nitrogen atoms.**

***Index Terms*—graphene, molecular dynamics, nitrogen, shear strength, grain boundary**

I. Introduction

CARBON materials have contributed the weight saving of the air frames, vehicle bodies and sports gears owing to their superior mechanical properties. However, the additional improvement in cost performance has been requested to expand the range of applications. Graphene, which is basic structure in carbon materials, has been found to have excellent tensile strength (~130 GPa) and the same Young's modulus (~1 TPa) as that of diamond. Therefore, more studies on graphene have recently increased in number [1]. Carbon materials contain various types of defects, namely, vacancies [2],[3], dislocations [4], sp^3-type defects [3], grain boundaries (GBs) [5] and heteroatoms [6]. It is crucial to clarify the relations between those defects and the mechanical properties of graphene to develop high-performance carbon materials.

Carbon materials derived from raw materials often contain impurities such as oxygen, nitrogen, or hydrogen atoms, and these impurities may affect the mechanical and electronic properties of the materials. Recently, Shen *et al*. [7] investigated the effects of nitrogen (N) doping on the mechanical properties of ultrananocrystalline diamond (UNCD) films, using molecular dynamics (MD) simulations. We performed the MD simulations on tensile loading of N-containing graphene in order to investigate the effect of N-atoms on mechanical properties of graphene in our previous paper [8]. It was found that N-atoms had little effect on the tensile properties of graphene except when two nitrogen atoms contained in graphene adjoined each other. The tensile properties of graphene with GBs were investigated by Grantab *et al*. using molecular simulations [9]. J. Han *et al*. have reported that the tensile strength of graphene with asymmetric tilt GBs shows tendency to increase as the misorientation angle rises [10]. The shear properties of pristine graphene were estimated by Min *et al* [11]. However, the shear properties of graphene with N-atoms and GBs have not been clarified so far. In our previous work, we investigated the influence of N-atom on the mechanical properties of graphene under shear loading, via MD simulations [12]. In addition, we clarified the shear properties of graphene containing both N-atoms and GBs using MD simulations. In this study, we also investigated the effect of adjoining N-atoms on the shear properties of graphene containing both N-atoms and GBs.

Manuscript received May 10, 2014. This work was supported in part by the Ring-Ring project of JKA.

Shingo Okamoto is with the Graduate School of Science and Engineering, Ehime University, 3 Bunkyo-cho, Matsuyama 790-8577, Japan (e-mail: okamoto.shingo.mh@ehime-u.ac.jp).

Akihiko Ito is with the Composite Materials Research Laboratories, Toray Industries, Inc., Masaki-cho 791-3193, Japan (e-mail: Akihiko_Ito@nts.toray.co.jp).

II. Method

A. Potential Functions

In the present study, we used two types of interatomic potentials: the second-generation reactive empirical bond order (2^{nd} REBO) [13] and Tersoff [14], [15] potentials. The 2^{nd} REBO potential for covalent C–C bonds is given by (1):

$$E_{REBO} = \sum_i \sum_{j>i} \left[V_R\left(r_{ij}\right) - B_{ij}^* V_A\left(r_{ij}\right) \right]. \quad (1)$$

The terms $V_R(r_{ij})$ and $V_A(r_{ij})$ denote the pair-additive interactions that reflect interatomic repulsions and attractions, respectively. The B_{ij}^* denotes the bond-order term.

The Tersoff potential for covalent C–N bonds is given by (2):

$$V = \frac{1}{2} \sum_{i \neq j} \left[f_C\left(r_{ij}\right) A_{ij} \exp\left(-\lambda_{ij} r_{ij}\right) - b_{ij} f_C\left(r_{ij}\right) B_{ij} \exp\left(-\mu_{ij} r_{ij}\right) \right], \quad (2)$$

where the parameter b_{ij} is the bond-order term that depends on the local environment.

$$b_{ij} = \chi_{ij} \left(1 + \beta^{n_i} \zeta_{ij}^{n_i}\right)^{-1/2n_i} \quad (3)$$

$$\zeta_{ij} = \sum_{k \neq i,\, j} f_C(r_{ik}) g(\theta_{ijk}) \quad , \tag{4}$$

$$g(\theta_{ijk}) = 1 + \frac{c_i^2}{d_i^2} - \frac{c_i^2}{d_i^2 + (h_i - \cos\theta_{ijk})^2} \quad , \tag{5}$$

where θ_{ijk} is the angle between bonds ij and ik.

The parameters A_{ij}, B_{ij}, λ_{ij}, and μ_{ij} depend on the atom type, namely, carbon or nitrogen. For atoms i and j (of different types), these parameters are

$$A_{ij} = (A_i \times A_j)^{\frac{1}{2}}, \; B_{ij} = (B_i \times B_j)^{\frac{1}{2}} \tag{6}$$

$$\lambda_{ij} = \frac{(\lambda_i + \lambda_j)}{2}, \; \mu_{ij} = \frac{(\mu_i + \mu_j)}{2} \quad , \tag{7}$$

where the parameters with a single index represent the interaction between atoms of the same type.

The parameter χ_{ij} in (3) takes into account the strengthening or weakening of the heteropolar bonds. There is no data for the determination of χ_{ij} for C–N interaction at present. In our model, this $\chi_{C\text{-}N}$ is set to 0.8833 to obtain the lattice constants a and b of the graphitic-C_3N_4 orthorhombic structure as 4.10 and 4.70 Å, respectively similar to the previous work [8]. From discussions on the N–N interaction, we know that the N molecule does not interact with other atoms, because of its high binding energy (9.8 eV) and that it diffuses through the crystal and exits the surface. In our model, to keep the nitrogen molecule stable inside the crystalline structure, $\chi_{N\text{-}N}$ is set to zero [7], [15].

In this work, the cutoff length $R_{\min}$ in the cutoff function $f_C(r)$, given by (8) of both the 2nd REBO and the Tersoff potentials is set to 2.1 Å to avoid the dramatic increase in interatomic forces similar to the method in our previous paper [8].

$$f_c(r) = \begin{cases} 1, & r < R_{\min} \\ \left\{ 1 + \cos\left[\dfrac{\pi(r - R_{\min})}{R_{\max} - R_{\min}} \right] \right\} / 2, & R_{\min} < r < R_{\max} \\ 0, & r > R_{\max} \end{cases} . \tag{8}$$

B. *Analysis model*

The analysis model of pristine graphene employed under the shear loading of armchair direction consists of 588 carbon atoms with dimensions identical to those of a real crystallite in typical carbon fibers [16], as shown in Fig. 1(a). In the case of the shear loading of zigzag direction, the analysis model consists of 576 carbon atoms with the same dimensions, as shown in Fig. 1(b).

The analysis model of graphene containing the tilt GB under the shear loading consists of 730 carbon atoms as shown in Fig. 2. There are many possible GB angles (the angles represent the total mismatch angle between the left and right grains) for graphene models with GBs. In the present study, we adopted the model with the GB angle of 21.7 ° which has the largest tensile strength among the models with each GB angle [9]. In this case, the five-membered rings and seven-membered ones are present in the GB.

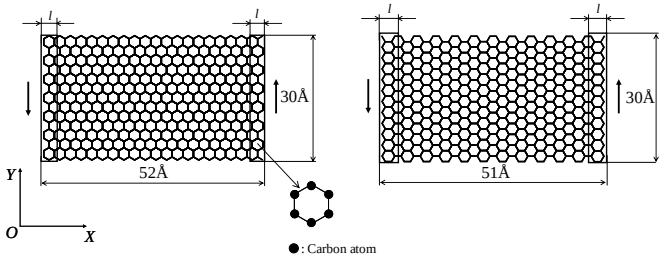

(a) Armchair direction (b) Zigzag direction

Fig. 1. Configuration of pristine graphene without GBs used under shear loading

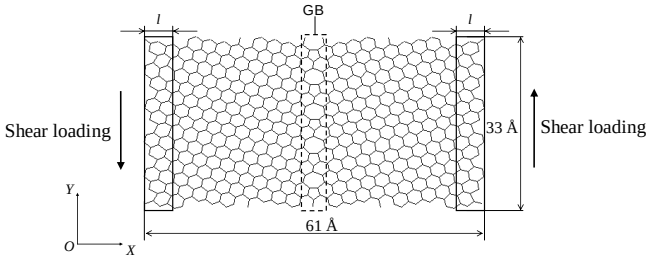

Fig. 2. Configuration of graphene containing armchair GBs with the GB angle of 21.7° used under shear loading.

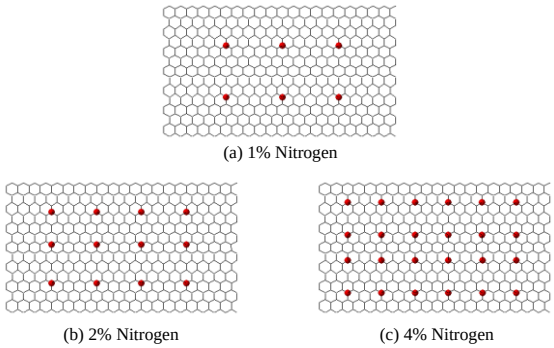

(a) 1% Nitrogen

(b) 2% Nitrogen (c) 4% Nitrogen

Fig. 3. Analysis models for N--containing graphene at each N-contents.

The periodic boundary condition is imposed in only the Y direction in the calculations of shear loading. The analysis models consist of two parts. One part is referred to as the active zone, in which the atoms move according to their interactions with neighboring atoms. The other part enclosed by the boxes as shown in Figs. 1 and 2 is referred to as the boundary zone, in which the atoms are restrained. The thickness l of the boundary zone is $1.5 \times \sqrt{3}a$ and $1.5a$ for the model without GBs used under shear loadings in the armchair and zigzag directions, respectively, where a is the length of C=C bond of graphene. The l of the analysis model with the GB is 4.23 Å.

The analysis models for uniformly distributed N-atoms in graphene are shown in Fig. 3. The carbon atoms in the active zone of the graphene model used in the armchair direction, as shown in Fig. 1(a), are replaced with the N-atoms such that the distance between neighboring N-atoms can be consistently uniform.

Three cases with differing N-contents, namely, 1 %, 2 %, and 4 %, are investigated.

In the analysis models of randomly distributed N-atoms in graphene, random carbon atoms in the active zone are replaced with N-atoms using pseudorandom numbers so that any

N-atoms can not adjoin each other.

C. MD simulation

All the MD calculations employ the velocity Verlet method to calculate the time integral of the equations of motion of atoms. The velocities of all atoms are adjusted simultaneously using the velocity scaling method [17] in order to control the temperature of the analysis models by the preset temperature T_{SET}. The mass of carbon atoms, m_C, and the mass of N-atoms, m_N, are 1.9927×10^{-26} kg and 2.3253×10^{-26} kg, respectively. The time step is 0.2 fs.

The atomic stress acting on each atom is calculated to obtain the stress–strain curves and visualize stress distribution during shear loadings. The atomic stress σ^i_{IJ} which is a component in the J direction in the I-plane is given by calculating the kinetic energies of, the interatomic force acting on, and the volume occupied by atom i, as given in (9):

$$\sigma^i{}_{IJ} = \frac{1}{\Omega^i}\left(m\overline{V^i{}_I V^i{}_J} + \overline{I^i F^i{}_J}\right), \tag{9}$$

where, Ω^i denotes the volume occupied by atom i, which is referred to as the atomic volume. This volume is calculated by averaging the volume of all atoms in the initial structure of each system. The m can be either m_C or m_N. The $F^i{}_J$ denotes the interatomic force acting on atom i from the neighbouring atoms. The global stress of an analysis model is calculated by averaging over all atoms in each system.

The initial positions of the atoms are given such that the analysis model can become identical to the crystal structure of N-containing graphene at 300 K. First, the atoms of the analysis model are relaxed until the stresses are stabilized for 14,000 MD simulation steps. The atoms in the active zone are relaxed in all the directions. The atoms in the left-hand side boundary zone are relaxed in only the Y direction. The atoms in the right-hand side one are relaxed in only the X and Y directions. After the atoms are relaxed, constant displacements are applied to the atoms in the boundary zones to calculate the shear loading in the Y direction. The atoms in the boundary zones are restrained in all the directions. The atoms in the active zone of the analysis model are relaxed for all the directions for 7,000 MD simulation steps. The shear strain increment $\Delta\gamma_{XY}$ is 0.0023. The shear moduli are obtained from the slopes of the straight lines in the range, where the relation between the stress and strain is linear, and the shear strengths are given by the peak of the nominal stress–nominal strain curves.

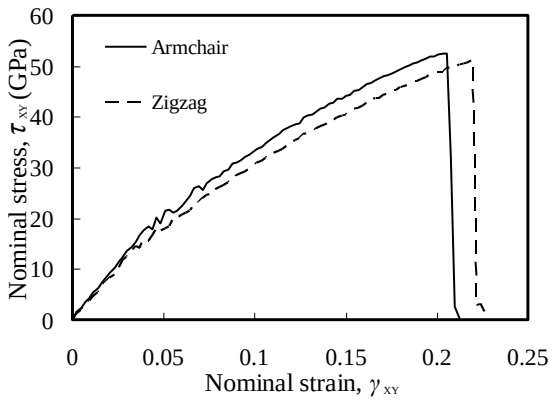

Fig. 4. Stress-strain curves of pristine graphene under shear loading.

TABLE I
SHEAR PROPERTIES OF PRISTINE GRAPHENE

Direction	Shear strength (GPa)	Shear modulus (GPa)
Armchair	53	442
Zigzag	51	408
Average	52	425

III. RESULTS AND DISCUSSION

A. Validation of calculation method

We performed the MD simulations on shear loadings of pristine graphene at 300 K to verify the propriety of our calculation method. The results of shear loadings are shown in Table I and Fig. 4. The average shear strength is 52 GPa, which nearly agrees with the 60 GPa calculated by Min *et al*. [11] using MD simulations. The average shear modulus is 425 GPa, which also nearly agrees with the experimentally obtained value of 434 GPa by Blakslee *et al*. [18].

B. Shear properties of nitrogen-containing graphene without GBs

MD simulations on shear loadings were performed in order to investigate the effect of N-atoms on the shear properties of graphene without GBs. In all the MD calculations, the shear loadings were applied in the armchair direction using the analysis model as shown in Fig. 1(a). Examples of the stress-strain curves of graphene containing uniformly distributed N-atoms are shown in Fig. 5. The calculated shear strengths and moduli are listed in Table II.

It was found that the shear strength and modulus of the graphene sheet do not change much with a change in the N-content.

Snapshots taken during the shear loadings are shown in Fig. 6. In all the cases, fractures occur because of cleavage of the C–C bond, which is in proximity to a C–N bond. This behavior was also found during the tensile loadings as reported in our previous paper [8].

Examples of the stress-strain curves of graphene containing randomly distributed N-atoms that do not adjoin each other, are shown in Fig. 7. The calculated shear strengths and moduli are listed in Table III. The shear strength and modulus do not change much with a change in the N-content.

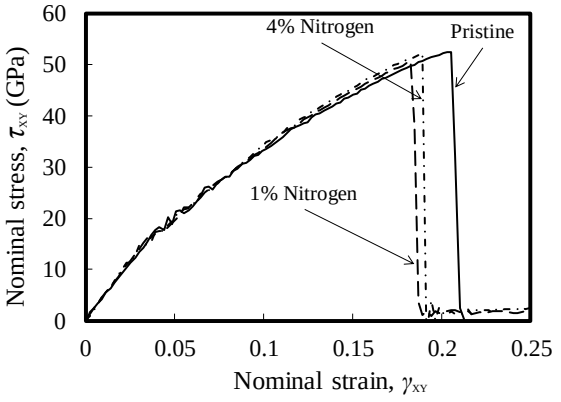

Fig. 5. Stress-strain curves of graphene containing uniformly distributed N-atoms.

TABLE II
SHEAR PROPERTIES OF GRAPHENE CONTAINING UNIFORMLY DISTRIBUTED N-ATOMS

Nitrogen content (%)	Shear strength (GPa)	Shear modulus (GPa)
0	53	442
1	51	458
2	51	473
4	52	477

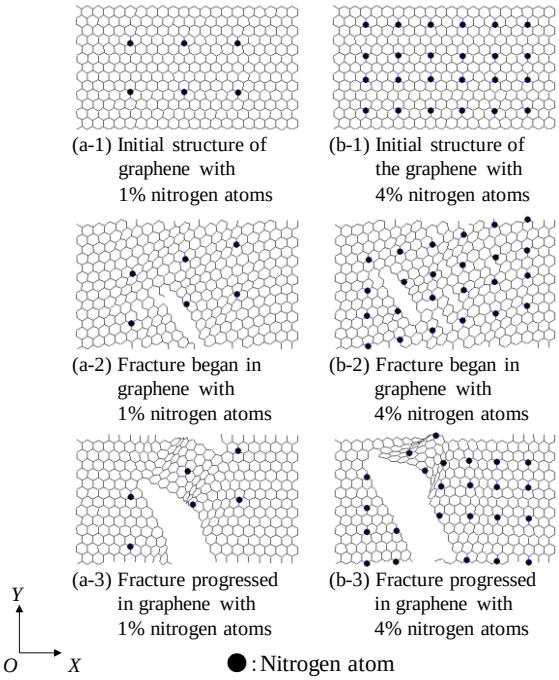

Fig. 6. Structures before tensile loading and after fracture for graphene containing uniformly distributed N-atoms at each N-content. 1 % nitrogen ((a-1)–(a-3)), 4 % nitrogen ((b-1)–(b-3)).

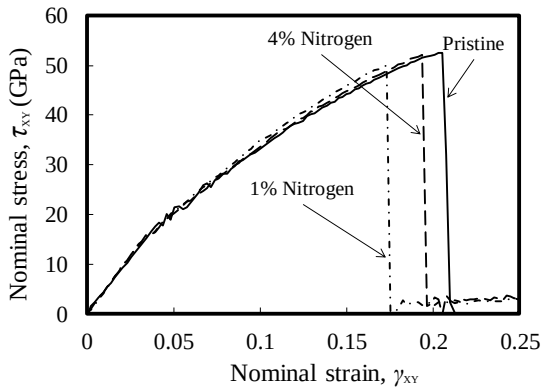

Fig. 7. Stress-strain curves of graphene containing randomly distributed N-atoms that do not adjoin each other.

TABLE III
SHEAR PROPERTIES OF GRAPHENE CONTAINING RANDOMLY DISTRIBUTED N-ATOMS THAT DO NOT ADJOIN EACH OTHER

Nitrogen content (%)	Shear strength (GPa)	Shear modulus (GPa)
0	53	442
1	52	465
2	51	479
4	50	466

Snapshots taken during the shear loadings are shown in Fig. 8. Fractures occur because of cleavage of the C-C bond, which is in proximity to a C-N bond. Those results are similar to the case of graphene containing uniformly distributed N-atoms.

Examples of the stress-strain curves of graphene containing randomly distributed N-atoms and including two adjoining ones are shown in Fig. 9. The calculated shear strengths and shear moduli are listed in Table IV. The decline in shear strength is larger than in the case of the random distribution in which N-atoms do not adjoin each other.

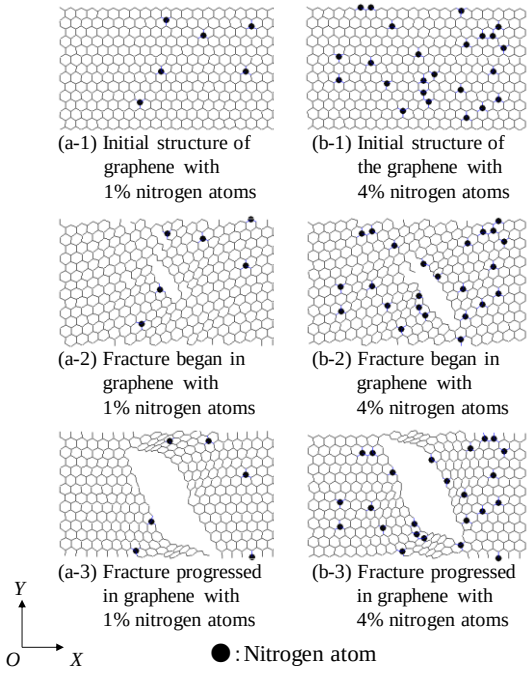

Fig. 8. Structures before shear loading and after fracture for graphene containing randomly distributed N-atoms that do not adjoin each other at each N-content. 1 % nitrogen ((a-1)–(a-3)), 4 % nitrogen ((b-1)–(b-3)).

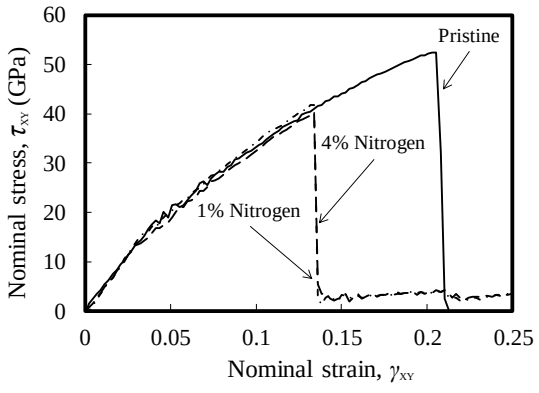

Fig. 9. Stress-strain curves of graphene containing randomly distributed N- atoms and including two adjoining ones.

TABLE IV
SHEAR PROPERTIES OF GRAPHENE CONTAINING RANDOMLY DISTRIBUTED N-ATOMS AND INCLUDING TWO ADJOINING ONES

Nitrogen content (%)	Shear strength (GPa)	Shear modulus (GPa)
0	53	442
1	40	452
2	41	462
4	42	466

Snapshots taken during the shear loadings are shown in Fig. 10. In all the cases, fracture occurs at the point where two N-atoms adjoin each other (marked by the circle), similar to the case of tensile loading as previously reported by the authors [8].

The relation between the shear strength and the N-content is shown in Fig. 11. The shear strength in the case of the randomdistribution including two adjoining N-atoms is lower than that in the other cases when N-content is over 1 %. From these results, it was found that the presence of two adjoining N-atoms in graphene affect the shear strength considerably. Then, those results are similar to the case of tensile loading.

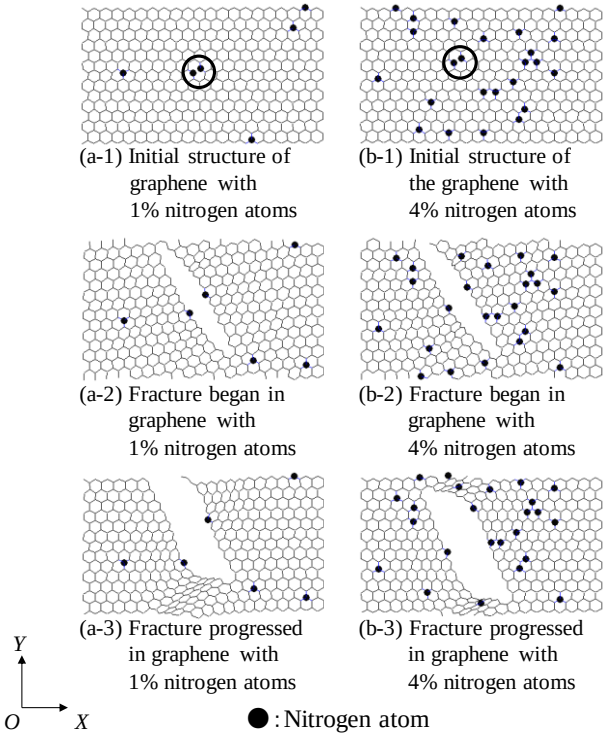

Fig. 10. Structures before shear loading and after fracture for graphene containing randomly distributed N-atoms at each N-content and including two adjoining ones. 1 % nitrogen ((a-1)–(a-3)), 4 % nitrogen ((b-1)–(b-3)).

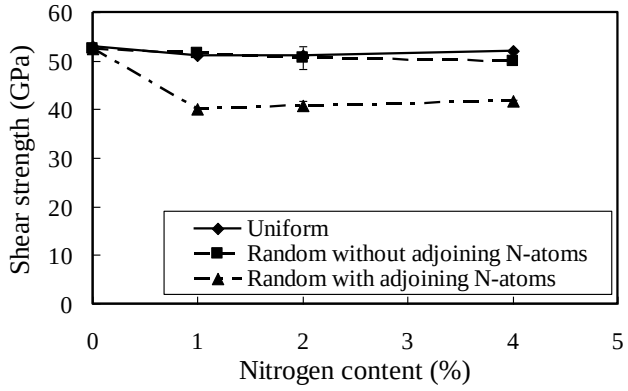

Fig. 11. Shear strength with N-content in graphene containing N-atoms on each distribution.

C. Shear properties of nitrogen-containing graphene with GBs

MD simulations on shear loadings of graphene containing the tilt GB and N-atoms were performed in order to investigate the effect of GBs and N-atoms on the mechanical properties of graphene. Examples of the stress-strain curves of graphene containing the tilt GB and randomly distributed N-atoms without adjoining N-atoms are shown in Fig. 12. The calculated shear strengths and moduli are listed in Table V.

It was found that the shear strength slightly decreases when the N-content is 4 %.

Snapshots taken during the shear loadings of graphene containing the tilt GBs without N-atoms are shown in Fig. 13.

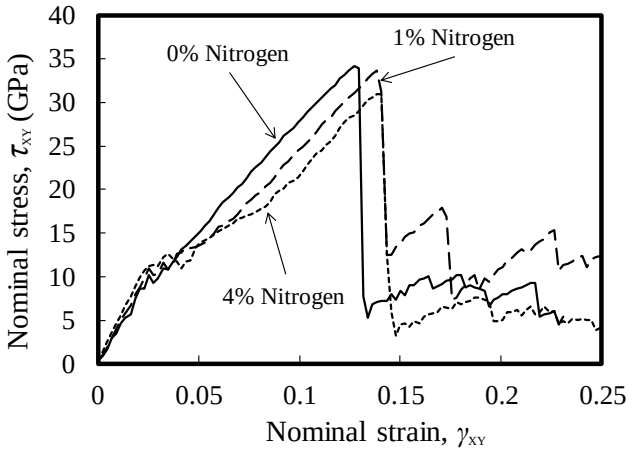

Fig. 12. Stress-strain curves of graphene containing the armchair GB and randomly distributed N-atoms without adjoining N-atoms.

TABLE V
SHEAR PROPERTIES OF GRAPHENE CONTAINING THE ARMCHAIR GB AND RANDOMLY DISTRIBUTED N- ATOMS WITHOUT ADJOINING N-ATOMS

Nitrogen content (%)	Shear strength (GPa)	Shear modulus (GPa)
0	34	390
1	34	412
4	31	460

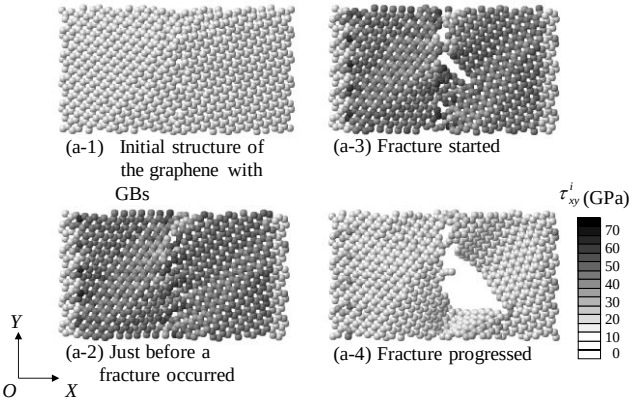

Fig. 13. Stages of fracture progress in graphene containing the armchair GB without N-atoms.

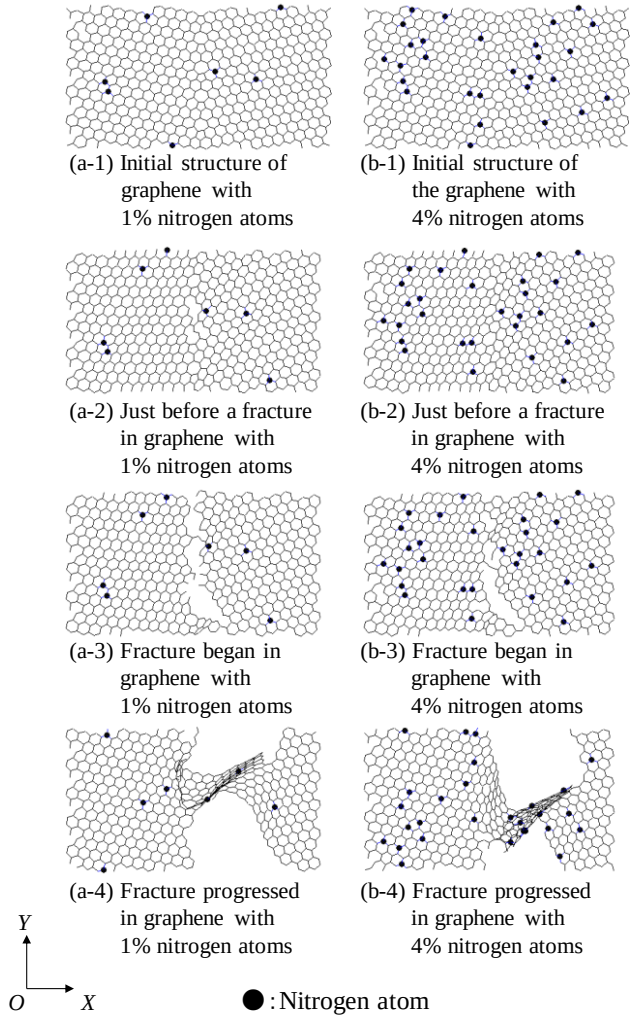

Fig. 14. Stages of fracture progression in graphene containing the armchair GB and ramdomly distributed N-atoms at each N-content without adjoining N-atoms. (a-1)–(a-4): 1 % nitrogen, (b-1)–(b-4) : 4 % nitrogen.

The shear stress concentrates around the GB, especially on the seven-membered rings. A fracture began at that point and progressed in the right hand side of the sheet. The direction of fracture progression is zigzag one, similar to the case of graphene without the GB. However, the fracture does not progress in the left hand side of the sheet differing to the case of graphene without the GB.

Snapshots of graphene containing the tilt GB and randomly distributed N-atoms without adjoining N-atoms are shown in Fig. 14. Fractures begin at the GB and not at the C-C bond, which is in proximity to a C-N bond differing to the case of graphene without the GB.

On the other hand, the calculated shear strengths and shear moduli of graphene containing the GB and randomly distributed N-atoms with two adjoining N-atoms are listed in Table VI. In addition, the relation between shear strength and N-content is shown in Fig. 15, together with the result in the case of not including adjoining N-atoms.

It was found that the shear strength slightly decreases as the N-content increses from 0 to 4 %, similar to the case of not including adjoining N-atoms.

TABLE VI
SHEAR PROPERTIES OF GRAPHENE CONTAINING THE ARMCHAIR GB AND RANDOMLY DISTRIBUTED N- ATOMS WITH TWO ADJOINING N-ATOMS

Nitrogen content (%)	Shear strength (GPa)	Shear modulus (GPa)
0	34	390
1	35	413
4	32	449

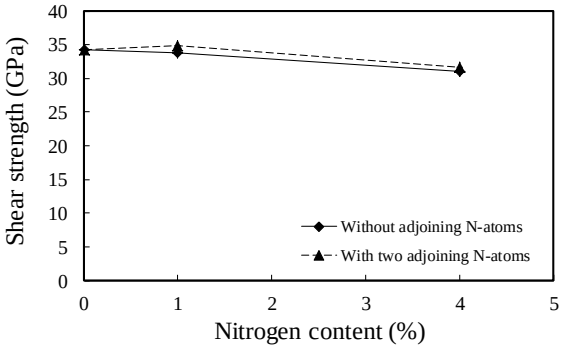

Fig. 15. Shear strength with N-content in graphene containing GB and N-atoms.

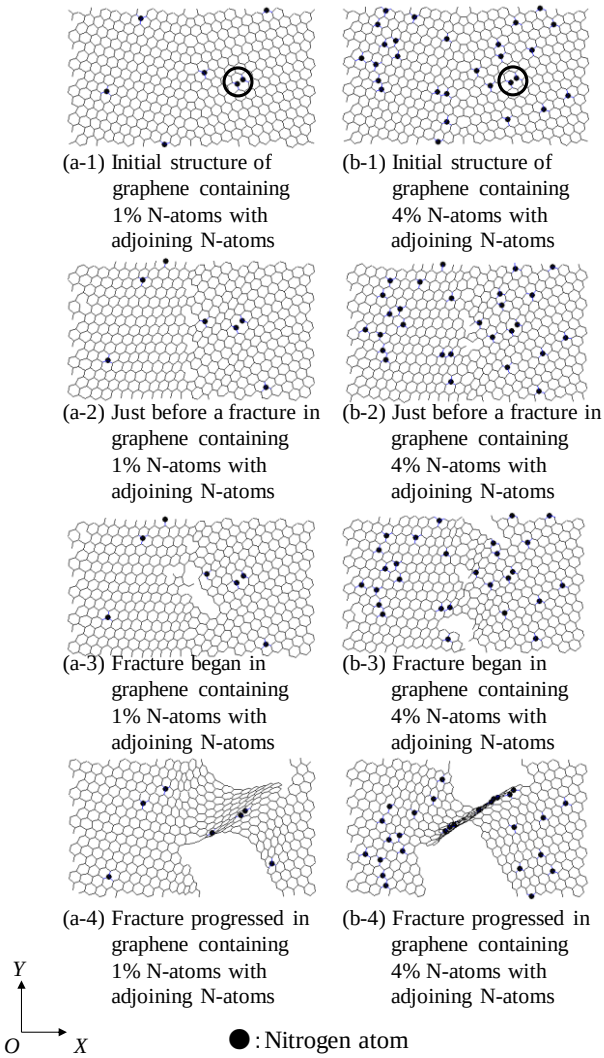

Fig. 16. Stages of fracture progression in graphene containing the armchair GB and ramdomly distributed N-atoms at each N-content with two adjoining N-atoms. (a-1)–(a-4): 1 % nitrogen, (b-1)–(b-4) : 4 % nitrogen.

The snapshots of graphene containing the GB and randomly distributed N-atoms with two adjoining N-atoms (marked by the circles) are shown in Fig. 16. The fractures begin at the GB even if the adjoining N-atoms exist.

In conclusion, the strength of graphene depends more greatly on the GB than N-atoms, whether two N-atoms present in graphene adjoin each other or not.

IV. Conclusion

We performed MD simulations on shear loadings of graphene containing N-atoms and the grain boundary (GB) in order to investigate the effect of the N-atom and GB on the shear properties of graphene. As a result, it was found that in the case of graphene without the GB both the shear strength and modulus do not change much for N-content of up to 4 %, unless two N-atoms present in graphene adjoin each other. Those results were similar to the case of tensile loading previously reported by the authors. Then, the shear strength of graphene is affected more extensively by the GB than N-atoms, whether two N-atoms present in graphene adjoin each other or not. .

References

[1] C. Lee, X. Wei, J. W. Kysar, J. Hone, "Measurement of the Elastic Properties and Intrinsic Strength of Monolayer Graphene," *Science*, vol. 321, pp. 385-388, Jul., 2008.

[2] P. A. Thrower, "The Study of Defects in Graphite by Transmission Electron Microscopy," *Chemistry and Physics of Carbon*, vol.5, pp. 217, 1969.

[3] A. Zandiatashbar, G-H. Lee, S. J. An, S. Lee, N. Mathew, M. Terrones, T. Hayashi, C. R. Picu, J. Hone, and N. Koratkar, "Effect of Defects on the Intrinsic Strength and Stiffness of Graphene," *Nature Communications*, vol. 5, Jan., 2014.

[4] A. Hashimoto, K. Suenaga, A. Gloter, K. Urita, and S. Iijima, "Direct Evidence for Atomic Defects in Graphene Layers," *Nature*,vol.430, pp.870-873, Aug., 2004.

[5] J. Osing and I. V. Shvets, "Bulk Defects in Graphite Observed with a Scanning Tunnelling Microscope," *Surface Science*, vol.417, pp.145–150, Nov., 1998.

[6] V. Serin, R. Fourmeaux, Y. Kihn, and J. Sevely, "Nitrogen distribution in high tensile strength carbon fibres," *Carbon*, vol. 28, pp. 573–578, 1990.

[7] L. Shen and Z. Chen, "An investigation of grain size and nitrogen-doping effects on the mechanical properties of ultrananocrystalline diamond films," *International Journal of Solids and Structures*, vol. 44, pp. 3379–3392, May, 2007.

[8] S. Okamoto and A. Ito, "Effects of Nitrogen Atoms on Mechanical Properties of Graphene by Molecular Dynamics Simulations," *Engineering Letters*, vol.20, pp. 169–175, May, 2012.

[9] R. Granatab, V. B. Shenoy, and R. S. Ruoff, "Anomalous strength characteristics of tilt grain boundaries in graphene," *Science*, vol. 330, pp. 946–948, Nov., 2010.

[10] J. Han, S. Ryu, D. Sohn, and S. Im, "Mechanical strength characteristics of asymmetric tilt grain boundaries in graphene," *Carbon*, vol. 68, pp. 250-257, Mar., 2014

[11] K. Min and N. R. Aluru, " Mechanical properties of graphene under shear deformation," *Applied Physics Letters*, vol.98, pp. 013113-1–013113-3, Jan., 2011.

[12] S. Okamoto and A. Ito, "Shear Properties of Graphene Containing Nitrogen Atoms and Grain Boundaries Using Molecular Dynamics Simulations," *Lecture Notes in Engineering and Computer Science: Proceedings of The International MultiConference of Engineering and Computer Scientists 2014 Vol I*, IMECS 2014, 12-14 Mar., 2014, Hong Kong, pp.529-534.

[13] D. W. Brenner, O. A. Shenderova, J. A. Harrison, S. J. Stuart, B. Ni, and S. B. Sinnott, "A second-generation reactive empirical bond order (REBO) potential energy expression for hydrocarbons," *Journal of Physics*: *Condensed Matter*, vol. 14, pp. 783–802, Jan., 2002.

[14] J. Tersoff, "Modeling solid-state chemistry: interatomic potentials for multicomponent systems," *Physical Review B*, vol. 39, no. 8, pp.5566–5568, Mar., 1989.

[15] J. Tersoff, "Structural properties of amorphous silicon nitride," *Physical Review B*, vol. 58, no. 13, pp. 8323–8328, Oct., 1998.

[16] D. J. Johnson, Handbook of polymer-fibre composites, Longman Publishing Group (1994) 24-29.

[17] L. V. Woodcock, "Isothermal molecular dynamics calculations for liquid salts," *Chemical Physics Letters*, vol. 10, pp. 257–261, Aug., 1971.

[18] O. L. Blakslee, D. G. Proctor, E. J. Seldin, G. B. Spence, T. Weng, Elastic constants of compression - annealed pyrolytic graphite, *Journal of Applied Physics*, vol. 41, pp. 3373–3382, Jul., 1970.